

Potential Of Soft Magnetic Powders For Shaded Pole Motor Design

Vasilija J. Sarac, Lidija B. Petkovska, Goga V. Cvetkovski and Zlatko B. Kolondzovski

Ss. Cyril and Methodius University, Faculty of Electrical Engineering P.O. Box 574, 1000 Skopje, Macedonia

E-mail: vasilija.sarac@siemens.com.mk; lidijap@eff.ukim.edu.mk; gogacvet@eff.ukim.edu.mk

Abstract: A shaded pole motor prototype is thoroughly examined. Weak points in the design are improved by using the method of Genetic Algorithm (GA), as powerful tool of optimization. In the new derived optimal models of motor, the static electromagnetic torque and efficiency factor are increased. Afterwards, some parts are built of soft magnetic powders (SMPs) and the design of the motor is improved. By using FEM in time harmonic domain, all derived models of the motor under consideration are profoundly analyzed. The best solutions and conclusions are proposed.

Keywords: Shaded pole motor, Genetic Algorithms, Time-harmonic Finite Element Method, Soft Magnetic Powders.

I. INTRODUCTION

The paper presents an extension of authors' previous works in the application of Genetic Algorithm – GA, as a powerful tool for optimization of electrical machines in general, as well as of the shaded pole motor in particular [1]-[3]. At the beginning, the optimization procedure was done at constraints imposed by the producer of the motor, i.e. at a condition of unchangeable radial cross-section geometry of the motor. The results related with two new optimal models, derived by using electromagnetic torque and efficiency factor as target functions are presented in [3]. Later, the work has been extended to development of new models, optimized with the same target functions as previous, but at much less constrains of the stator pole geometry. The derived optimal models are OMM1 and OMM2, respectively. The results of optimization are presented in the next section. The torque at rated speed and the efficiency in the optimal models are improved. Knowing that performance of the new stator core leads to a costly product, a potential of soft magnetic powders (SMPs) is examined. It is proposed some parts to be built of soft magnetic powders, improving the design of the motor. These new improved motor models IMM1 and IMM2 are corresponding to the previously derived ones.

A deepened analysis of the all motor models, by using the results of magnetic field computations performed by time harmonic FEM is carried out.

II. THE OBJECT OF STUDY

In this paper as an object of study and investigation, a shaded pole motor type AKO-16 "MikronTech" product, is considered. Rated data are: $2p = 2$; $U_n = 220$ V; $f_n = 50$ Hz; $I_{1n} = 0.125$ A; $P_{1n} = 18$ W; $n_n = 2520$ rpm. This motor is adopted as a prototype, i.e. basic model – BMM. The geometrical cross section is presented in Figure 1.

In order to provide a reference for comparison of the gained results, this motor is thoroughly examined and the most interesting parameters and performance characteristics are determined [4].

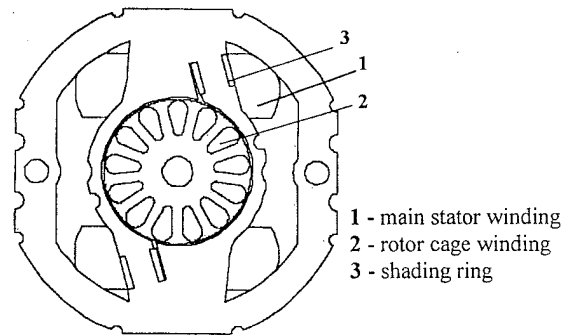


Figure 1: Cross section of the shaded pole motor

III. OPTIMIZATION PROCEDURE AND RESULTS

Aiming to the improvement of the shaded pole motor performance characteristics, an optimization procedure based on GA is carried out. Optimization variables are: core length n [mm], stator pole width b_p [mm], shading portion of pole a [p.u.], air-gap magnetic flux density B_δ [T], skewing angle of the rotor bars α_{sk} [deg.], current density of the stator winding Δ [A/mm²]. As could be expected, all windings parameters will be changed, too.

In separate input file of GA program, the range of variations of selected motor variables is defined. Basing on the experience and skills, the range of variation of the most important motor parameters mentioned above, is placed in the following constraints:

- Current density in the stator winding Δ (5÷10) [A/mm²];
- Core length n (10÷20) [mm];
- Magnetic flux density in the air-gap B_δ (0.4÷0.45) [T];
- Width of stator pole b_p (10÷20) [mm];
- Shading portion of stator pole a (0.2÷ 0.3) [p.u.];
- Angle of the rotor skewing α_{sk} (15÷20) [deg.].

As an output, the best set of varied parameters is obtained. The optimization results are presented in Table I.

TABLE I: OUTPUT RESULTS FOR CONSTRAINED PARAMETERS

| BMM | OMM1 | OMM2 |
|---------------------------------|---------------------------------|---------------------------------|
| $\Delta=8$ [A/mm ²] | $\Delta=5$ [A/mm ²] | $\Delta=5$ [A/mm ²] |
| $n=16$ mm | $n=18$ mm | $n=18$ mm |
| $B_\delta=0.404$ T | $B_\delta=0.45$ T | $B_\delta=0.40$ T |
| $b_p=16$ mm | $b_p=12$ mm | $b_p=12$ mm |
| $a=0.25$ | $a=0.2$ | $a=0.2$ |
| $\alpha_{sk}=17$ [deg.] | $\alpha_{sk}=10.023$ [deg.] | $\alpha_{sk}=10.023$ [deg.] |

During the optimization procedure, the GA based computer program is set up to create 6000 generations. When electromagnetic torque is used as target function, the first optimal motor mode OMM1 is obtained.

Afterwards, the optimization procedure is extended by developing another optimal motor model OMM2 with the same optimization variables, but with efficiency factor as target function [5].

In Table II is presented the comparison of parameters for the basic motor model – BMM and two developed optimal models – OMM1 and OMM2.

TABLE II: COMPARISON OF MOTOR PARAMETERS

| BMM | OMM1 | OMM2 |
|---------------------------------|---------------------------------|---------------------------------|
| $d_{Cu}=1.4 \cdot 10^{-4}$ [mm] | $d_{Cu}=1.8 \cdot 10^{-4}$ [mm] | $d_{Cu}=1.6 \cdot 10^{-4}$ [mm] |
| $W=3488$ turns | $W=2784$ turns | $W=3132$ turns |
| $R_1=492.98 \Omega$ | $R_1=245.3 \Omega$ | $R_1=341.12 \Omega$ |
| $X_1=498.17 \Omega$ | $X_1=904.67 \Omega$ | $X_1=1138.72 \Omega$ |
| $R_2=457.04 \Omega$ | $R_2=289.89 \Omega$ | $R_2=366.79 \Omega$ |
| $X_2=76.71 \Omega$ | $X_2=65.994 \Omega$ | $X_2=83.54 \Omega$ |
| $R_3=18,474 \Omega$ | $R_3=18,723 \Omega$ | $R_3=23,687 \Omega$ |
| $X_3=127.53 \Omega$ | $X_3=45.075 \Omega$ | $X_3=57.07 \Omega$ |
| $X_{12}=2,163.3 \Omega$ | $X_{12}=1,970 \Omega$ | $X_{12}=2,493 \Omega$ |
| $X_{13}=175.91 \Omega$ | $X_{13}=154.62 \Omega$ | $X_{13}=195.35 \Omega$ |

In accordance with Figure 1, the subscript “1” is used for description of the main stator winding parameters; “2” is linked to the rotor cage winding and “3” is corresponding to the short circuit coil (shading ring). The parameters of all shaded-pole motor windings are “seen” from the main stator winding side, i.e. they are calculated on the basis of W turns per pair of stator poles.

In Table III the comparison between characteristics at rated loading condition, meaning slip $s_n=0.16$, for the prototype motor, as well as for the optimal designed motor models is presented.

TABLE III: COMPARISON OF MOTOR CHARACTERISTICS

| Quantity | BMM | OMM1 | OMM2 |
|--|--------|--------|--------|
| Stator current I_1 [A] | 0.126 | 0.13 | 0.102 |
| Stator current density Δ [A/mm ²] | 8.1851 | 5.1087 | 5.0731 |
| Short circuit coil current I_3 [A] | 0.0063 | 0.0048 | 0.0038 |
| Rotor current I_2 [A] | 0.0878 | 0.101 | 0.0793 |
| Power factor $\cos\phi$ [/] | 0.654 | 0.47 | 0.481 |
| Input power P_1 [W] | 18.11 | 13.47 | 10.814 |
| Output power P_2 [W] | 4.15 | 4.511 | 3.373 |
| Efficiency factor η [/] | 0.229 | 0.335 | 0.32 |
| Electromagnetic torque M_{em} [mNm] | 18.075 | 19.447 | 15.365 |

From the data presented in Tables, it is evident that in both optimized model the stator winding current density is lower, as result of greater diameter of wire; at the same time, the number of turns in the main stator winding is decreased, leading to lower resistance of all windings. Finally, the torque and output power will be increased.

In Table IV are extracted only the values for static electromagnetic torque M_{em} [mNm] and efficiency η [/], in the both derived models OMM1 and OMM2, when M_{em} and η are accepted as target optimization functions, respectively. In the last row is presented their percentage improvement/change compared with values of BMM.

TABLE IV: COMPARISON OF OPTIMIZED TARGET FUNCTIONS

| BMM | | OMM1 | | OMM2 | |
|--|--------|----------------|--------|----------------|--------|
| M_{em} [mNm] | η | M_{em} [mNm] | η | M_{em} [mNm] | η |
| 18.075 | 0.229 | 19.447 | 0.335 | 15.365 | 0.32 |
| Improvement / change compared to the basic motor model [%] | | 7.59 | 46.29 | -14.99 | 39.74 |

For better understanding of the shaded pole motor behavior, it is recommended to continue with calculation and an analysis of the motor performance characteristics in the whole range of slip s ($0 \div 1$). In the previous works of the authors [4] they are presented in details.

On the basis of the optimization results and the values for parameters and characteristics presented in Tables II and III, the detailed performance analysis of the three models is carried out. In brief, the following comparisons and conclusions can be emphasized:

A. Motor Model OMM1: Target Function - Torque

- The number of turns of the main stator winding in OMM1 is less for 20.2% leading to an increase of current in the main stator winding. The fact that the current in the stator winding is greater, leads to a greater currents in other motor windings: shading coil and the rotor cage.

- Apart from this fact, the optimization procedure is resulting with improved efficiency of the motor, mainly because of significant decrease of windings' resistances.

- As expected, in the optimized motor model OMM1, electromagnetic torque at rated load point is increased, mostly because of an increase of input current in the main stator winding, as well as current in the rotor winding.

- On the other hand, because of the greater copper wire diameter, the current density is decreasing effectively. This is good achievement from an operational point of view; as copper losses in the motor are becoming lower, the efficiency factor will be higher, too.

- From all relevant performance characteristics of the shaded-pole motor, only the power factor $\cos\phi$ in the new derived model is lower; but for this special type of motor, the gained values, as are presented in Table III, are still considered to be satisfactory high.

- The angle of the rotor skewing is also changing, in accordance with the change of shading portion of poles.

B. Motor Model OMM2: Target Function - Efficiency

- The input current in the main stator winding in optimized model OMM2 is lower than in BMM, due to the increased reactive resistance of the winding; but, as active resistance is still lower than in BMM, the result is lower copper losses and improved efficiency factor.

- The number of turns of the main stator winding now is less for 10.2%, but the current in the winding is decreased. The explanation of this fact can be found in the influence of its value on the efficiency.
- Current density due to greater cooper wire diameter and lower current is decreased, resulting with lower heat losses and improved efficiency factor.
- The static electromagnetic torque at rated load point is lower, mostly because of the lower input currents in the main stator winding and, consequently, in the rotor winding, too. Emphasizing the fact that target function of optimization in this case is efficiency, not electromagnetic torque, the gained result is fully comprehensive.

C. Improved Models IMM1 and IMM2 with SMPs

The next step is the derivation of improved motor models, in which some parts of the stator core, i.e. poles and bridges are built of soft magnetic powders (SMPs). These two improved solutions are selected to be IMM1 and IMM2, respectively to the previously derived ones, with two different target functions of optimization. The adjustment is carried out only on the stator geometry, with respect to output results from two GA optimization procedures. The new design is performed easy, by simply substitution of the magnetic material in the stator core.

The analysis is now extended to these new models. For this purpose, the Finite Element Method is applied [6]. The most interesting results of calculations are presented comparatively, in the following heading.

IV. FINITE ELEMENT ANALYSIS

The Finite Element Method is contemporary numerical method which enables to calculate distribution of magnetic flux density in any machine cross section, thus enabling to plot magnetic field distribution inside the object of investigation. It is usually used as a non-linear magnetostatic problem which is solved in the terms of magnetic vector potential **A**. However, when analyzing induction machines, considering their AC excitation, the air-gap magnetic field is always a time-varying quantity. In materials with non-zero conductivity eddy currents are induced; consequently, the field problem turns to magnetodynamic, becoming the non-linear time harmonic problem [7].

Even more, when rotor is moving, its quantities are oscillating at slip frequency, quite different from the stator frequency, and the direct implementation of the non-linear time harmonic analysis is improper. The problem is solved by adjusting the rotor bars conductivity σ , corresponding to the slip. Hence, the non-linear time harmonic analysis, by using FEM, is performed at fixed stator current supply frequency $f=50\text{Hz}$, while the rotor slip is changing with load. In that case, the following partial equation is going to be solved numerically:

$$\nabla \times \left(\frac{1}{\mu(B)} \nabla \times A \right) = -\sigma A + J_{src} - \sigma \nabla V \tag{1}$$

where J_{src} represents the applied current sources.

A. Basic Motor Model – BMM

The FEM analysis of the shaded pole motor prototype, as well as the derived models with optimal and improved design, is starting with the motor prototype BMM. Three different motor regimes, as the most interesting are considered: no-load and slip $s=0$; rated load at slip $s=0.16$; locked-rotor with slip $s=1$. They are presented in Figure 2, (a), (b) and (c), respectively.

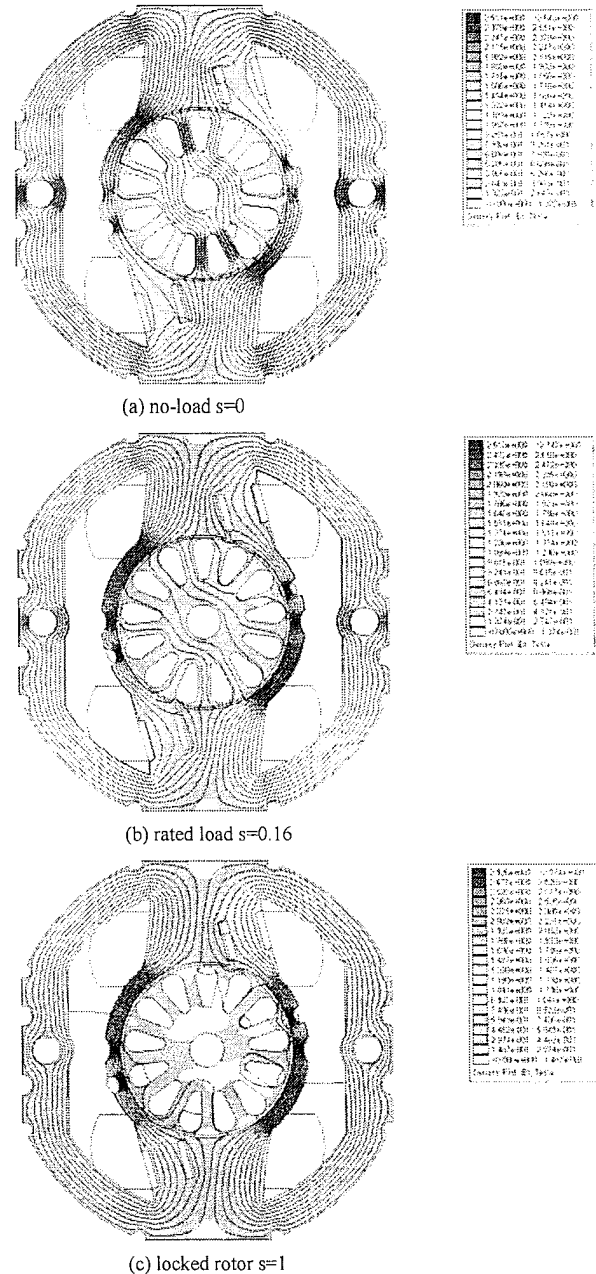


Figure 2: Magnetic field distribution in the motor prototype – BMM

The effect of the induced field from current in the rotor cage winding on the main stator field is evident. Although the overall maximum value of the magnetic flux density is increasing with an increase of the slip, the distribution of the magnetic field in the cross section of the motor is more uniform and with obviously less intensity.

B. Optimal Motor Models OMM1 and OMM2

The new developed design of the shaded pole motor under consideration, derived by GA optimization procedure carried out with two different target functions, are thoroughly examined and analyzed in the heading III. Here will be presented comparatively the computational results obtained by using FEM, for the same operating regimes as in the previous subheading, concerning the motor prototype. In Figures 3, is presented the working regimes at no-load, meaning the slip $s=0$. Here bellow in the figures, (a) is related with motor model optimally designed with electromagnetic torque as target function, and (b) is related with the optimally designed model at efficiency as target function.

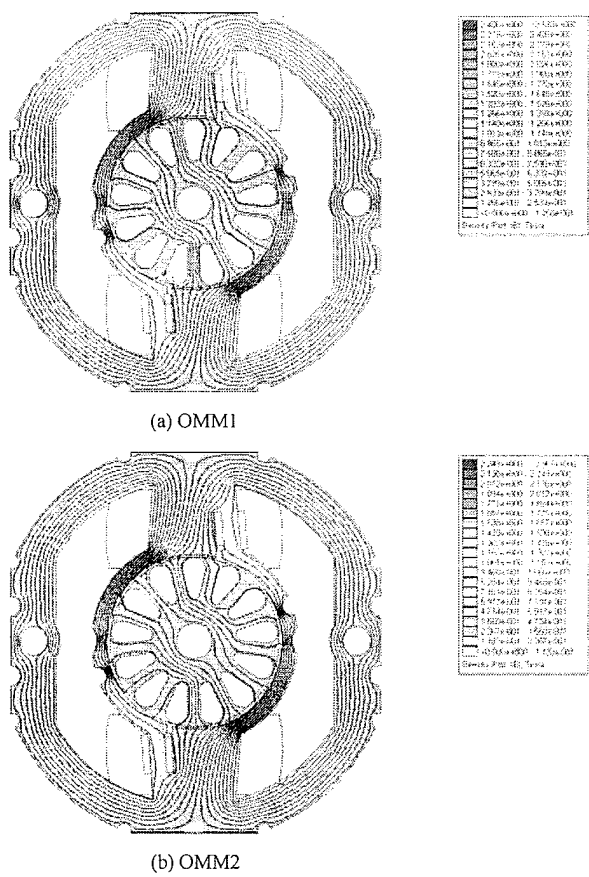


Figure 3: Magnetic field distribution at no-load $s=0$ in the GA optimized motor models

In the above presented figures, the effect of the optimization procedure performed on the prototype of the shaded pole motor is evident. Although the main stator winding input current is increasing the overall maximum value of the magnetic flux density is decreasing due to the new geometrical arrangement of the motor design.

In Figures 4 and 5, there are presented the working regimes at rated load and at stand still, respectively. Here bellow, (a) and (b) are related with the new optimally designed motor models in the same sense as previously.

On the basis of an analysis of the figures presented in continuation, the similar and corresponding conclusions for the magnetic field behavior could be drawn.

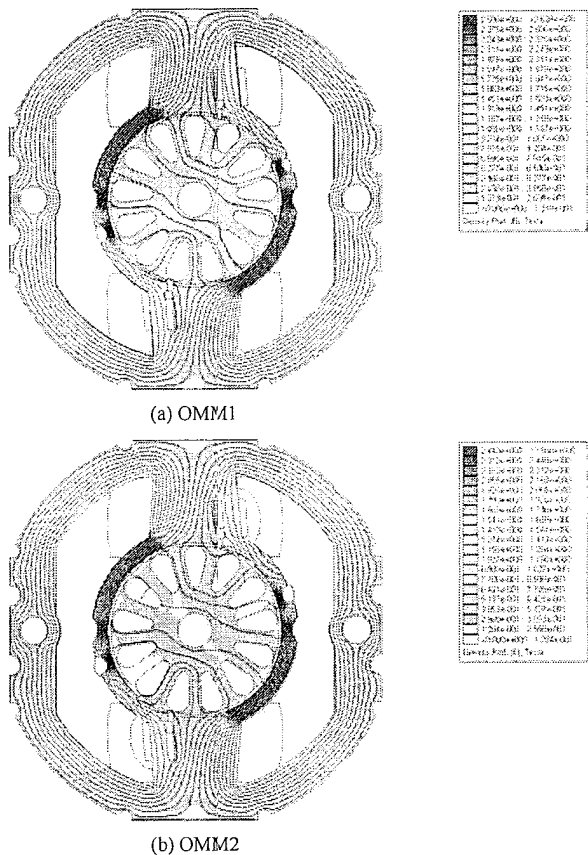


Figure 4: Magnetic field distribution at rated load $s=0.16$ in the GA optimized motor models

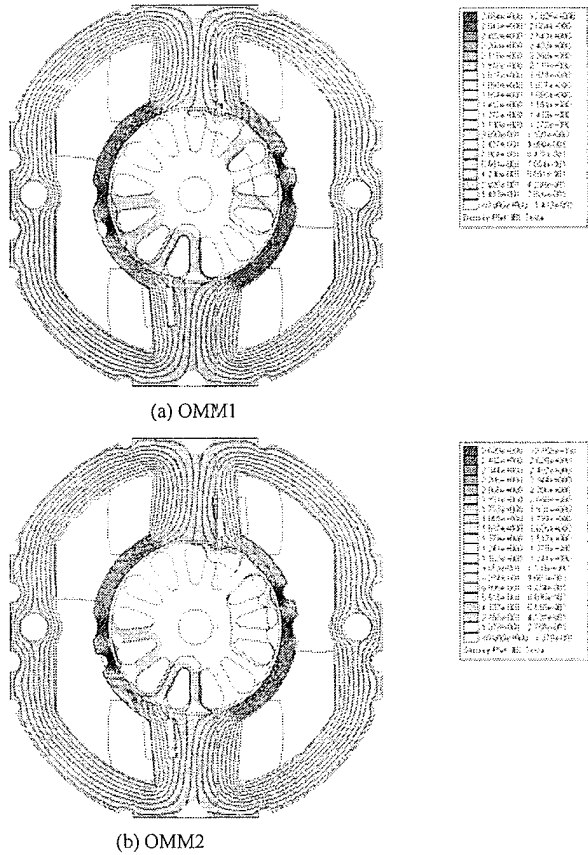
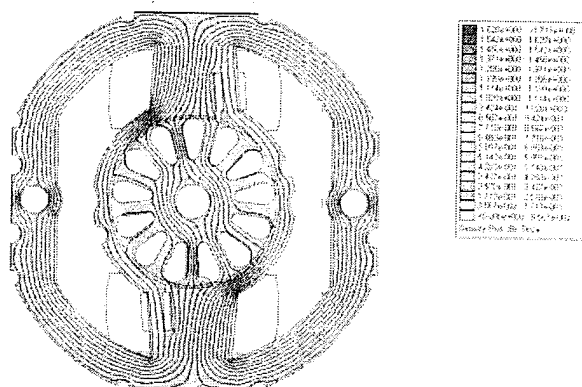


Figure 5: Magnetic field distribution at locked rotor $s=1$ in the GA optimized motor models

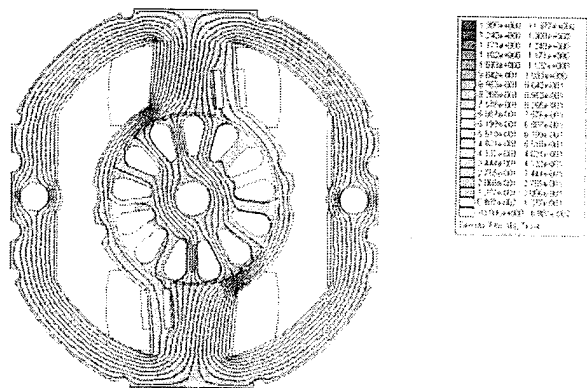
C. Improved Models IMM1 and IMM2 with SMPs

Knowing that manufacturing of new designed stator core always means a costly product, we propose to use soft magnetic powders (SMPs) instead of thin magnetic steel sheets. This operation is especially suitable knowing the fact that soft magnetic powders are with high magnetic quality and are easily shaped. As stator poles and bridges are designed to be detachable from the yoke, we propose to replace only these parts of the stator core.

On the basis of optimal model OMM1 is developed an improved model IMM1, and the optimal model OMM2 is linked with another improved model IMM2. The Finite Element Method is used again, and the magnetic field distribution at the same working regimes is calculated. The potential of soft magnetic powders is examined.

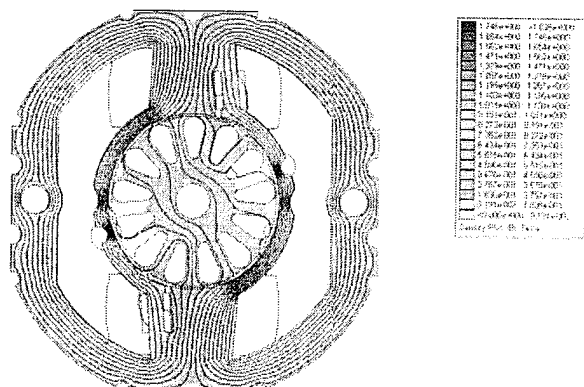


(a) IMM1

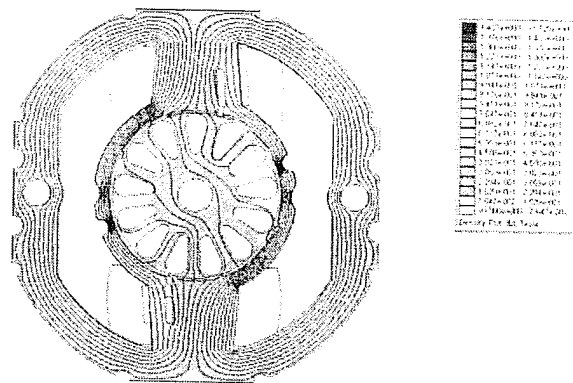


(b) IMM2

Figure 6: Magnetic field distribution in improved models at no load

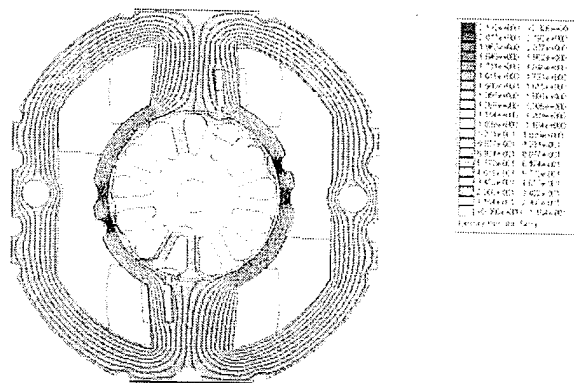


(a) IMM1

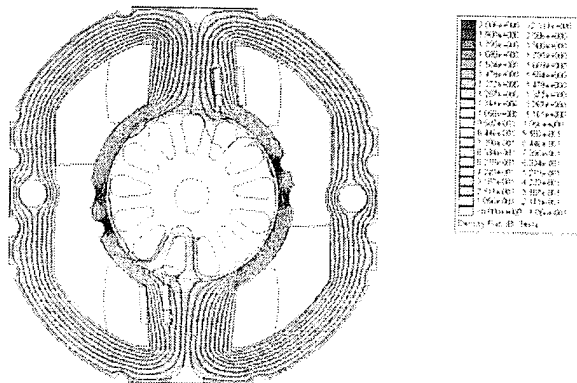


(b) IMM2

Figure 7: Magnetic field distribution in improved models at rated load



(a) IMM1



(b) IMM2

Figure 8: Magnetic field distribution in improved models at stand still

V. PERFORMANCE ANALYSIS

Analyzing the above figures, one can notice that SMPs use in the motor design, leads to lower flux densities, i.e. lower iron saturation especially in motor critical parts such as stator bridges. As the most interesting, for all studied models at all working regimes, the iron losses are calculated and presented in Table V.

TABLE V: COMPARISON OF IRON LOSSES

| | Iron losses [W] | | | | |
|--------|-----------------|--------|--------|--------|-------|
| | BMM | OMM1 | IMM1 | OMM2 | IMM2 |
| s=0 | 0.3435 | 0.2895 | 0.0775 | 0.2083 | 0.708 |
| s=0.16 | 0.236 | 0.2473 | 1.43 | 0.1907 | 0.878 |
| s=1 | 0.1972 | 0.2153 | 1.76 | 0.1775 | 1.286 |

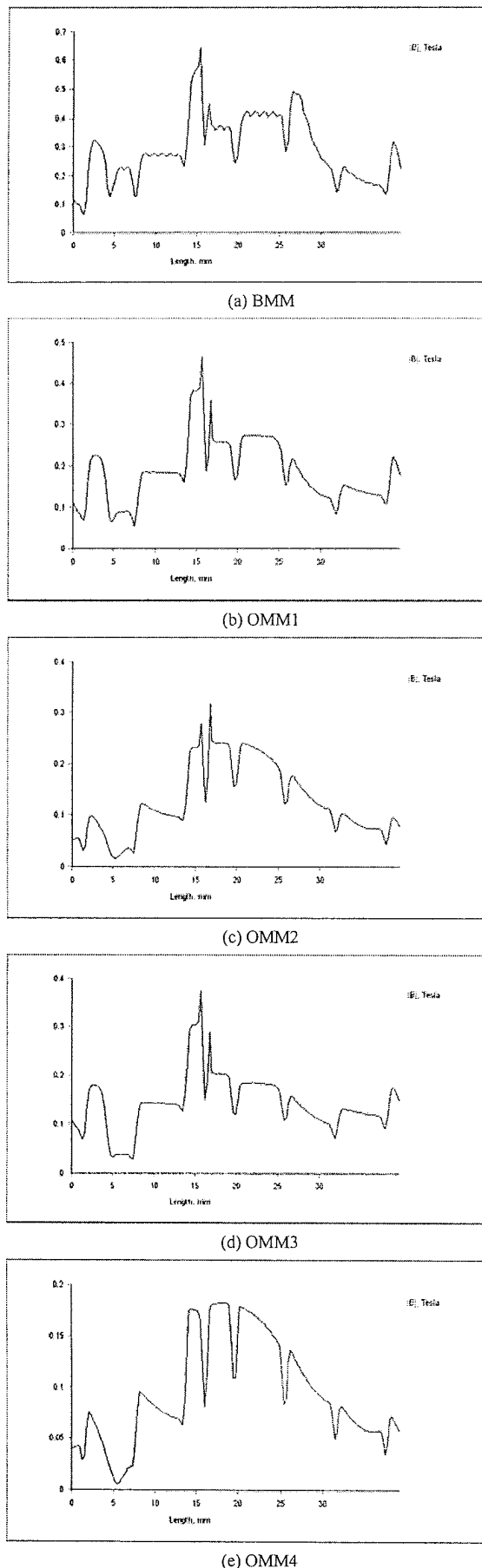


Figure 9: Spatial distribution per pole at rated load $s=0.16$

It is evident that soft magnetic powders produce iron loss of greater value, although the overall magnetic field is weakened. Only this outcome is discussible.

In Figure 9 is presented spatial distribution of magnetic flux density along one pole pitch at rated load, for all considered motor models. For easier examination of the results, the derived models are presented simultaneously.

VI. CONCLUSIONS

In the paper an original study of the shaded pole motor design based on GA method is presented. Optimization procedure is performed by changing stator pole geometry of the prototype motor, accepted as basic model – BMM. Two target functions are in use, and two optimal motor models OMM1 and OMM2 are derived. Afterwards, an improvement of the design, by using SMPs is done and another two models IMM1 and IMM2, closely linked to the previous ones, are proposed. Prototype and all derived models are analyzed using FEM. Main conclusions are:

- Motor design OMM1 derived when target function is electromagnetic torque is increasing its value for 7.6 %, at the simultaneous efficiency increase of 46.29 %. The model OMM2 when target function is efficiency is resulting with an increase of its value for 39.7 %, but it must be emphasized at a decrease of torque.
- FEM analysis shows that in all derived motor design, magnetic flux density is lower, contributing to lower iron saturation. After, by using SMPs for manufacturing of the stator poles and bridges, the lower flux density in these parts is obtained.
- Due to the particular SMPs properties, the improved design of motor models result with higher iron loss. Apart from this fact, it is not considered to be a disadvantage.

REFERENCES

- [1] G. Cvetkovski, L. Petkovska, M. Cundev, S. Gair: "GA Approach in Design Optimisation of a PM Disk Motor", *Journal COMPEL*, Vol. 19, No. 2, pp. 608-614, MCB Press London, United Kingdom, 2000.
- [2] L. Petkovska, G. Cvetkovski, V. Sarac: "Finite Element Method Coupled with Genetic Algorithm as a Design Optimization Tool of Electromagnetic Devices", *Short Papers Proceedings of the Symposium on Power Electronics, Electrical Drives, Automation & Motion – SPEEDAM'04*, Vol. 2/2, pages T2D 13-16, on CD pp. 606-611, Capri, Italy, 2004.
- [3] V. Sarac, L. Petkovska, G. Cvetkovski, "Comparison Between Two Target Functions for Optimization of Single Phase Shaded Pole Motor Using Method of Genetic Algorithms", *Book of Digests of the 3rd Japanese-Mediterranean Workshop on Applied Electromagnetic Engineering for Magnetic and Superconducting Materials – JAPMED'03*, pp. 43-44, Athens, Greece, 2003.
- [4] V. Sarac, L. Petkovska: "A Novel Approach to Performance Characteristics Evaluation of Shaded Pole Induction Motor", *Journal ELECTROMOTION*, Vol. 10, No. 3, pp. 205-210, 2003.
- [5] V. Sarac, L. Petkovska, M. Cundev, G. Cvetkovski, "GA Based Optimal Design of a Shaded Pole Motor", *Accepted paper for the International conference of Electrical Machines – ICEM'04*, to be held 5-8 September 2004, Krakow, Poland.
- [6] David Meeker, "Finite Element Method Magnetics," *User's Manual, FEMM*, Version 4.0, Waltham, Boston, MA, USA, 2004.
- [7] V. Sarac, L. Petkovska, M. Cundev: "Non-linear Time Harmonic Analysis of Shaded Pole Micromotor", *Proceedings of the International Symposium on electromagnetic Fields in Electrical Engineering – ISEF'03*, Vol. 1/2, pp. 137-142, Maribor, Slovenia, 2003.